

Remix the Timbre: Diffusion-Based Style Transfer Across Polyphonic Stems

Leduo Chen, Junchuan Zhao[†], Shengchen Li

lec015@ucsd.edu, Junchuan@u.nus.edu, Shengchen.Li@xjtlu.edu.cn

Abstract

Timbre transfer aims to modify the timbral identity of a musical recording while preserving the original melody and rhythm. While single-instrument timbre transfer has made substantial progress, existing approaches to multi-instrument settings rely on separate-then-transfer pipelines that propagate source separation artifacts and produce incoherent synthesized timbres across stems. This paper proposes MixtureTT, to the best of our knowledge the first system for flexible per-stem timbre transfer directly from a polyphonic mixture. Given a mixture and a separate timbre reference for each target voice, MixtureTT jointly transfers all stems to the specified instruments through a shared diffusion process. Modeling the dependencies across the per-stem content and cross-stem harmonic, the proposed joint stem diffusion transformer eliminates cascaded separation error, reduces inference cost by a factor equal to the number of stems, and yields more coherent multi-stem outputs. Despite operating under a strictly harder input condition, evaluations on the SATB choral dataset show that MixtureTT outperforms single-instrument baselines on both objective and subjective metrics demonstrating the necessity of dedicated multi-instrument timbre transfer over the naive separate-then-transfer pipelines. As a result, this work confirms that the cross-stem modeling is essential for mixture-level timbre transfer as the proposed joint setting consistently exceeds an equivalent single-stem ablation. Audio samples are available at supporting webpage ¹.

Index Terms: timbre transfer, source separation

1. Introduction

Timbre transfer is a form of music style transfer in which the perceptual identity of an instrument is recast onto the musical content of another, while pitch, rhythm, and articulation are preserved. Modeling timbre is notoriously difficult: as the attribute that distinguishes instruments playing the same note at the same loudness and duration, it manifests as heterogeneous, source-dependent patterns across time and frequency [1].

Most prior work on timbre transfer has focused on the single-instrument setting, where both the content source and the timbre reference are isolated monophonic recordings. Early systems based on autoregressive waveform models [2, 3] and adversarial translation [4, 5, 6] were succeeded by VAE-based methods [7, 8, 9] and, most recently, by diffusion-based approaches [10, 11, 12, 13] that now define the state of the art. Multi-instrument timbre transfer remains comparatively under-explored: existing mixture-level systems either treat the full ensemble as a single timbral unit [14, 15], permitting only

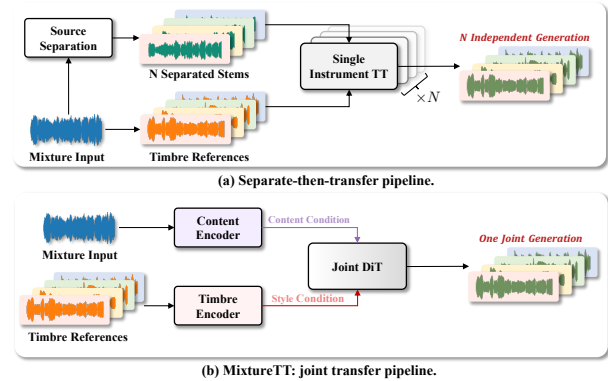


Figure 1: **Top:** the separate-then-transfer pipeline forced by single-instrument tools. **Bottom:** MixtureTT performs joint per-stem transfer directly from the mixture.

fixed ensemble-to-ensemble conversion, or require external per-source query audio to enable source-level control [16]. To our knowledge, no existing method extracts per-stem content implicitly from a polyphonic mixture, assigns an independent target timbre to each voice, and performs all transfers jointly in a single pass.

This gap matters because musicians rarely work with isolated stems, and a producer typically receives a stereo bounce rather than separated tracks. When the goal is to re-instrument a mixture itself, yet a practitioner aiming for per-stem transfer with today’s tools is forced into a *separate-then-transfer* pipeline: run a source separator to recover individual stems, then apply a single-instrument transfer model to each in turn. This workaround is a downstream consequence of the field’s single-instrument focus and carries three compounding drawbacks. Separation introduces modeling error that propagates into every transfer step; the diffusion model runs once per stem, scaling both training and inference cost with the number of voices; and because the per-stem runs proceed independently, neither the harmonic relationships binding the voices nor the acoustic consistency of a shared timbral space can be enforced. The ensemble is reconstructed stem by stem rather than as an integrated whole (Fig. 1).

To fill this gap, this paper proposes **MixtureTT**, a system that performs per-stem timbre transfer through joint denoising of all stems within a shared diffusion trajectory. Given a polyphonic mixture and one timbre reference per target voice, MixtureTT generates every re-instrumented stem in parallel: each reverse-diffusion step updates all stems through one network call, amortizing the per-stem cost of separate-then-transfer.

[†]indicates the corresponding author.

¹https://mixturett.github.io/Mixture_TT/

The central component is a *Joint Stem Diffusion Transformer* whose three-stage attention design balances per-stem independence with cross-stem coordination, allowing attention to propagate harmonic structure and timbral coherence directly during denoising—two forms of inter-stem coherence that independent per-stem passes have no mechanism to recover. Our contributions are as follows:

- We propose MixtureTT, to our knowledge the first system for per-stem timbre transfer directly from a polyphonic mixture, without explicit source separation or per-source query audio.
- On the SATB choral benchmark, MixtureTT outperforms strong single-instrument diffusion baselines on both objective and subjective metrics, despite taking the mixture rather than isolated stems as input.
- A controlled ablation against a matched single-stem variant shows that joint denoising is essential—not merely cheaper—for capturing the cross-stem dependencies that mixture-level timbre transfer requires.

2. Related Work

2.1. Single-instrument Timbre Transfer

Single-instrument timbre transfer has evolved through three paradigms. Early audio-to-audio translation methods, including WaveNet-based autoregressive decoders with domain confusion losses [3] and CycleGAN pipelines on time-frequency representations [4, 14], demonstrated cross-instrument conversion but suffered from limited fidelity and one-to-one constraints. A second line introduced explicit content-timbre disentanglement via self-supervised VQ-VAE representations [7] and factorized latent spaces [8], enabling many-to-many transfer with one-shot references. Most recently, diffusion models have come to dominate [10, 11, 15, 12], with adversarial disentanglement of structural and timbral information [11] and unsupervised diffusion bridges between instrument domains [12] representing the current state of the art. Despite this progress, every method in this line assumes a monophonic single-instrument input and cannot operate directly on polyphonic mixtures.

2.2. Mixture-level Timbre Manipulation

Research on manipulating mixtures directly remains scarce, and existing efforts fall into two limited categories. The first treats the entire mixture as an atomic timbral unit: GAN-based [14] and diffusion-based [15] mixture-to-mixture pipelines transfer one ensemble configuration to another, but cannot manipulate individual voices and are restricted to fixed ensemble pairs seen during training. The second permits source-level manipulation at the cost of additional input requirements: DisMix [16], the closest prior work, extracts per-source pitch and timbre latents via a query-conditioned encoder, but requires external query audio for source identification and operates only within or between complete mixtures. Beyond timbre transfer specifically, multi-source diffusion models [17] jointly model multiple stems in a single diffusion process for unconditional composition and separation, demonstrating that joint stem modeling is feasible with diffusion, but they do not address conditional re-instrumentation of an existing mixture under content-fidelity constraints.

2.3. Diffusion Models for Audio Generation

Diffusion models [18, 19] have become the dominant paradigm for generation tasks, and latent diffusion [20] extends this

paradigm to the compressed latent space of a pretrained autoencoder, with strong audio adaptations [21, 22]. MixtureTT builds on this line by adopting the EDM preconditioning [23, 22] as our latent backbone and apply classifier-free guidance [24] independently on the content and timbre conditions during training.

3. Method

MixtureTT decompose each musical signal into a time-varying content space (melody, rhythm, articulation) and a time-invariant timbre space (instrument identity), and recombine them at inference through a joint latent diffusion process over N stems ($N=4$ for the SATB choral data used in our experiments). Fig. 2 shows the full pipeline.

3.1. Audio Codec

Audio codecs are widely used in audio generation and conversion, as they map raw waveforms into compact latent representations [21, 25, 26, 27, 28]. Following [11], our audio codec is a convolutional autoencoder following the RAVE design [29], featuring the adversarial discriminator of [30]. It compresses a raw waveform \mathbf{x} into an latent sequence $\mathbf{z} \in \mathbb{R}^{L \times D_z}$, where L is the time dimensions and D_z is the embedding space. The codec is pretrained on our dataset and frozen throughout. The subsequent diffusion model operate on the codec latents \mathbf{z} space. Codec decoder maps the latents back to waveforms at inference.

3.2. Content Extraction

As content frontend the encoder of HT Demucs [31] is adopted, retrained on our data and frozen. HT Demucs natively produces two parallel streams—a frequency-domain branch capturing harmonic structure and a time-domain branch capturing transient and articulatory cues—both useful for disambiguating co-occurring voices. The mixture is fed into the encoder to obtain $\mathbf{z}_{\text{freq}} \in \mathbb{R}^{C \times F \times T_f}$ and $\mathbf{z}_{\text{time}} \in \mathbb{R}^{C \times T_t}$. Here $C=512$ is the shared bottleneck channel dimension; F, T_f denote the downsampled frequency and time dimensions of the spectrogram branch; T_t is the downsampled temporal length of the waveform branch.

A trainable Dual-Branch Content Adapter consumes both tensors. Each branch is processed independently with strided convolutions and residual blocks, the two streams are temporally aligned via pooling, and they are fused by channel-axis concatenation into a unified mixture-level feature. From this shared feature, $N=4$ stem-specific projection heads produce one content vector $\mathbf{c}^{(i)} \in \mathbb{R}^{L \times D_c}$ per target voice ($D_c=16$), with $i \in \{0, 1, 2, 3\}$ indexing the soprano, alto, tenor, and bass parts respectively. Because every $\mathbf{c}^{(i)}$ is read out from the same shared backbone and the adapter never materializes stem-level waveforms, our content path avoids the cascaded-error problem of separate-then-transfer pipelines.

3.3. Timbre Encoding and Disentanglement

Timbre encoder. For each stem i , the reference waveform is encoded by the frozen codec to $\tilde{\mathbf{z}}^{(i)}$, then processed by a 1D convolutional network with global average pooling, yielding $\boldsymbol{\tau}^{(i)} \in \mathbb{R}^{D_\tau}$ ($D_\tau=16$). During training, references are drawn from a different temporal window of the same track to encourage time-invariant encoding. At inference, any clip of the target instrument can serve as the reference, independent of the input

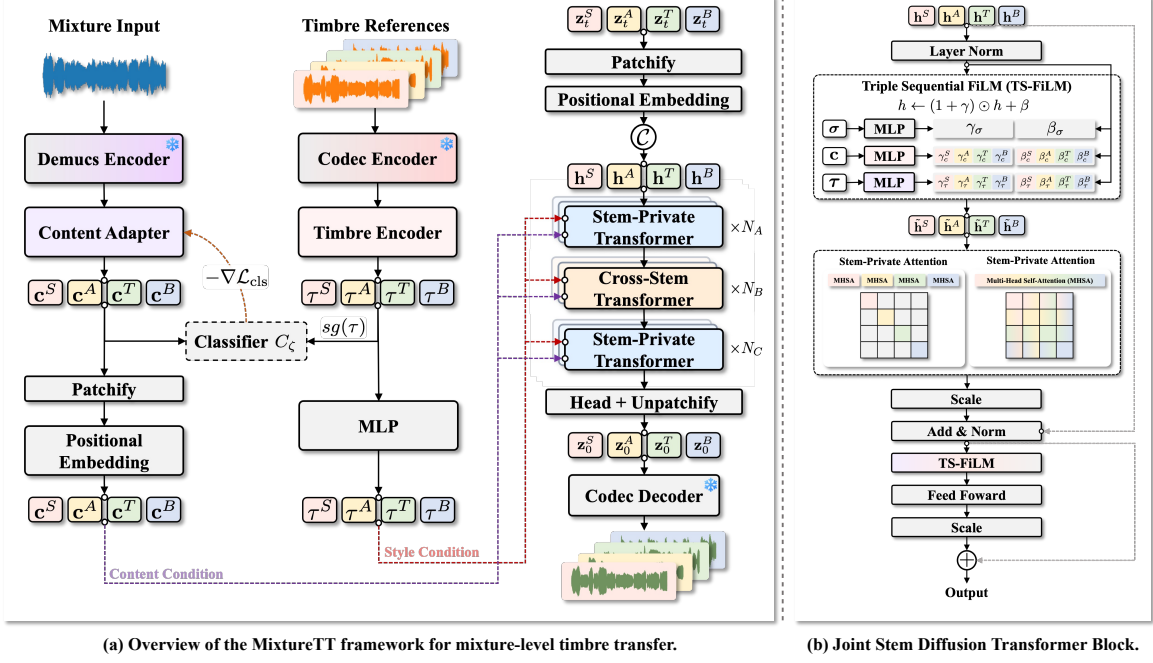


Figure 2: Overview of MixtureTT. The mixture is processed by a frozen Demucs encoder and a trainable dual-branch content adapter to produce per-stem content embeddings $\mathbf{c}^{(i)}$. Timbre references are encoded by the frozen codec and a timbre encoder into global embeddings $\tau^{(i)}$. The Joint Stem DiT denoises N noisy stem latents jointly through three stages (Intra-Stem \rightarrow Cross-Stem \rightarrow Refinement), conditioned on content and timbre via decoupled FiLM. The denoised latents are decoded back to waveforms by the frozen codec decoder.

mixture.

Disentanglement. Low-dimensional bottlenecks alone do not guarantee disentanglement [11]. Therefore an auxiliary classifier is trained $C_\zeta : \mathbb{R}^{L \times D_c} \rightarrow \mathbb{R}^{D_\tau}$ to predict the timbre embedding from the content vector,

$$\mathcal{L}_{cls} = \frac{1}{N_s} \sum_{i=1}^{N_s} \|C_\zeta(\mathbf{c}^{(i)}) - \text{sg}(\tau^{(i)})\|_2^2, \quad (1)$$

where $\text{sg}(\cdot)$ stops gradients. C_ζ minimizes Eq. 1 while the content encoder maximizes it, forcing $\mathbf{c}^{(i)}$ to discard timbre information.

To prevent timbre collapse, we apply two complementary penalties. First, a cross-stem term drives the four voice timbres toward mutual orthogonality within each mixture:

$$\mathcal{L}_{div}^{cross} = \frac{1}{|\mathcal{P}|} \sum_{(i,j) \in \mathcal{P}} \cos \text{sim}^2(\tau^{(i)}, \tau^{(j)}), \quad (2)$$

where $\cos \text{sim}(\mathbf{u}, \mathbf{v}) \triangleq \mathbf{u}^\top \mathbf{v} / (\|\mathbf{u}\|_2 \|\mathbf{v}\|_2)$ denotes cosine similarity and \mathcal{P} is the set of stem pairs. Second, a batch-variance term prevents the encoder from collapsing to an input-agnostic constant:

$$\mathcal{L}_{div}^{var} = \frac{1}{N_s} \sum_{i=1}^{N_s} \max(0, \delta - \text{std}_B(\tau^{(i)})), \quad (3)$$

where std_B is the standard deviation over the batch and δ a target threshold. The total diversity loss is $\mathcal{L}_{div} = \mathcal{L}_{div}^{cross} + \lambda_{var} \mathcal{L}_{div}^{var}$.

3.4. Joint Stem Diffusion Transformer

Running a single-instrument diffusion model independently on each stem incurs N_s -fold inference cost and offers no channel through which the N_s denoising trajectories can coordinate, leaving harmonic and timbral coherence across voices unenforced. We instead denoise all stems in one pass with a shared network F_θ , whose cost is independent of N_s .

Tokenization. Each stem latent $\mathbf{z}_i \in \mathbb{R}^{L \times D_z}$ is patchified along time with patch size $p=8$, linearly projected to dimension D , and added to learned positional embeddings, yielding $\mathbf{h}_i \in \mathbb{R}^{L' \times D}$ with $L'=L/p$. The N_s per-stem sequences are concatenated along the length axis into $\mathbf{h} \in \mathbb{R}^{N_s L' \times D}$ (64 tokens for $N=4, L'=16$), which is then processed by a stack of transformer blocks. During training, the stem ordering of the concatenation is randomly permuted and inverted at the output, blocking positional shortcuts to stem identity.

Three-stage attention. The block stack is partitioned into three stages that share an identical block design and differ only in the self-attention mask. Let $s(i) = \lfloor i/L' \rfloor$ denote the stem index of token i . Stages A ($\times N_A$) and C ($\times N_C$) use *intra-stem* attention, in which each token attends only to tokens of the same stem; concretely, the mask satisfies $M_{intra}[i, j] = 0$ when $s(i) = s(j)$ and $-\infty$ otherwise, yielding a block-diagonal attention pattern with N_s blocks of size $L' \times L'$. Stage B ($\times N_B$) removes the mask, letting every token attend across all stems. This ordering first builds clean per-voice representations, then opens a single dedicated channel for the cross-stem coordination that ensemble coherence requires, and finally refines each voice locally without re-introducing cross-talk.

Conditioning via decoupled FiLM. Each transformer block is conditioned on three signals—the diffusion timestep σ , the

per-stem content $\mathbf{c}^{(i)}$, and the per-stem timbre $\boldsymbol{\tau}^{(i)}$ —through three independent FiLM [32] pathways, extending the adaptive layer normalization of diffusion transformers [33]. For each signal $u \in \{\sigma, c, \tau\}$, a dedicated MLP produces modulation parameters (γ_u, β_u) applied sequentially to the pre-norm hidden state $h \in \mathbb{R}^{N_s L' \times D}$:

$$h \leftarrow (1 + \gamma_\tau) \odot \left[(1 + \gamma_c) \odot \left((1 + \gamma_\sigma) \odot h + \beta_\sigma \right) + \beta_c \right] + \beta_\tau. \quad (4)$$

Unlike the shared-projection fusion common in latent diffusion backbones [20, 22], the three pathways share no parameters, preventing weaker signals from being bottlenecked and keeping gradients to the timbre pathway well-conditioned even under strong content variation—a regime in which entangled FiLM is known to suppress style information [11]. As in standard DiT [33], attention and FFN residuals are gated by a σ -derived scalar initialized to zero. Content thus modulates what happens when within a voice, while timbre imposes a time-invariant identity across it. The final output is un-patchified and un-permuted to recover one denoised tensor per stem.

3.5. Training Objective

Following EDM [23], the joint denoiser F_θ is trained with the σ -weighted objective

$$\mathcal{L}_{\text{diff}} = \mathbb{E} \left[\frac{w(\sigma)}{N_s} \sum_{i=1}^{N_s} \left\| F_\theta(\mathbf{z}_t^{(i)}; \sigma, \mathbf{c}^{(i)}, \boldsymbol{\tau}^{(i)}) - \mathbf{z}_0^{(i)} \right\|_2^2 \right] \quad (5)$$

with σ drawn from a log-normal schedule, $\mathbf{z}_{t,i} = \mathbf{z}_{0,i} + \sigma \boldsymbol{\epsilon}_i$ for $\boldsymbol{\epsilon}_i \sim \mathcal{N}(0, \mathbf{I})$, and $w(\sigma)$ the standard EDM loss weighting. All N stems share a single σ per training step, so the joint model sees correlated noise levels across voices, consistent with their joint denoising at inference. The full training objective combines $\mathcal{L}_{\text{diff}}$ with the disentanglement losses of Sec. 3.3:

$$\mathcal{L} = \mathcal{L}_{\text{diff}} - \lambda_{\text{cls}} \mathcal{L}_{\text{cls}} + \lambda_{\text{div}} \mathcal{L}_{\text{div}}. \quad (6)$$

4. Experiments

4.1. Dataset

Experiments are conducted on the *tiny* partition of CocoChorales [34] (24k/8k/8k train/val/test at 16 kHz), which provides four-part (SATB) chamber renditions across three main ensemble categories and several random combinations, each accompanied by isolated stems and a pre-mixed mixture.

Two evaluation settings are considered. In *Reconstruction* (Rec.), each input stem serves as its own timbre reference, providing an upper bound on content preservation. In *Transfer* (Trans.), references are drawn from a different ensemble category (e.g., brass→strings) and paired with input mixtures through a fixed-seed shuffle for reproducibility.

4.2. Training Details

The audio codec is pretrained for 1M steps and then frozen. The joint diffusion model is trained for 400k steps with AdamW [35] at a constant learning rate of 1×10^{-4} and a batch size of 8 mixtures (equivalently 32 stem samples). Training takes roughly one day on a single NVIDIA RTX 5090.

Schedule. The first 25k steps form a timbre-warmup phase: content is replaced by a learned sentinel and the cross-stem stage is bypassed, preventing early collapse onto a content shortcut. Real content is then linearly faded in over 5k steps, after which all stages train jointly.

Decoupled CFG. Following [24], classifier-free guidance is extended to both conditions: content and timbre are dropped under separate Bernoulli masks at training, and inference uses two guidance scales w_c, w_τ to decouple content fidelity from timbre-transfer strength.

4.3. Baselines and Ablations

Baselines. Two single-instrument timbre transfer methods are used as baselines, both retrained on CocoChorales *tiny* with their official implementations. **SS-VAE** [7] disentangles timbre and content via a VQ-VAE and transfers timbre by swapping the style code. **Control-Transfer-Diffusion(CTD)** [11] conditions a latent diffusion model on pitch and loudness contours with a separate timbre encoder. Since neither accepts a polyphonic mixture, we run them on the ground-truth isolated stems provided by CocoChorales and mix the four transferred outputs to obtain a mixture-level result.

Ablations. Three ablations of MixtureTT are evaluated. Single DiT removes the cross-stem stage ($N_B=0$) and invokes the network once per stem, isolating the contribution of joint denoising under a matched architecture and parameter count. *w/o* \mathcal{L}_{cls} disables the adversarial content–timbre classifier, removing explicit disentanglement pressure. *w/o* \mathcal{L}_{div} disables the cross-stem diversity loss, allowing the four timbre embeddings to collapse toward each other.

4.4. Evaluation Metrics

Evaluation spans three dimensions, audio quality, content preservation, and timbre fidelity, at both stem and mixture levels. Audio quality is measured by **Fréchet Audio Distance** [36] over VGGish embeddings, reported at the stem level as **FAD** and the mixture level as **FAD_m**. Content preservation combines two metrics. **JD**, the **Jaccard Distance** on MIDI-quantized F0 contours extracted with pYIN [37], scores per-stem pitch preservation; codec-induced quantization imposes a nonzero lower bound on Rec. JD. **CCS**, the **Chroma Cosine Similarity** between CQT chromagrams of the input and generated mixtures, captures harmonic preservation at the ensemble level. Timbre fidelity is assessed from two complementary views. **MFCC**, the **MFCC Timbre Distance**, follows [7] in training a triplet network on MFCC coefficients 2–13 [38] on our dataset, embedding stems into a timbre space in which distance to the per-stem reference reflects perceptual dissimilarity. **Conf**, the **Classifier Confidence**, reports the mean softmax probability assigned to the target instrument by a 13-class CNN that we train on 64-band log-mel spectrograms of CocoChorales stems, providing a class-based counterpart.

4.5. Subjective Evaluation

An anonymous listening test was conducted with 35 participants comparing MixtureTT against SS-VAE and CTD, both run on ground-truth isolated stems. Each trial was rated on a five-point MOS scale along four axes. For per-stem axes, participants were shown a content source and a timbre reference, then the transferred stem, and rated (1) *Success in Transfer* (ST): timbre match to the reference; (2) *Content Preservation* (CP): melodic/rhythmic match to the content source; and (3) *Sound Quality* (SQ): overall audio quality. For the mixture-level axis, participants were shown a content mixture and the four timbre references, then the transferred mixture, and rated (4) *Inter-stem Coherence* (IC): harmonic, rhythmic, and dynamic alignment of the four voices as a unified ensemble—directly evaluating the

Table 1: *Objective evaluation on CocoChorales under self-reconstruction (Rec.) and cross-timbre transfer (Trans.) settings.*

		Per-Stem								Mixture			
		FAD↓		JD↓		MFCC-cos↓		Conf↑		FAD _m ↓		CCS↑	
		Rec.	Trans.	Rec.	Trans.	Rec.	Trans.	Rec.	Trans.	Rec.	Trans.	Rec.	Trans.
Baselines	SS-VAE [7]	0.536	0.643	0.204	0.302	0.028	0.047	0.984	0.830	0.596	0.763	0.961	0.896
	CTD [11]	0.541	0.605	0.161	0.177	0.017	0.068	0.068	0.766	0.549	0.573	0.960	0.955
Ablations	w/o \mathcal{L}_{cls}	<u>0.091</u>	0.272	<u>0.141</u>	<u>0.153</u>	0.012	0.051	0.988	0.356	0.063	0.294	<u>0.991</u>	0.980
	w/o \mathcal{L}_{div}	0.088	0.087	0.138	0.139	0.011	0.073	0.991	0.001	0.058	0.070	0.990	<u>0.990</u>
	Single-stem	0.102	0.304	0.166	0.287	<u>0.010</u>	<u>0.034</u>	0.988	<u>0.970</u>	0.061	0.227	0.985	0.933
MixtureTT	—	0.097	<u>0.255</u>	0.159	0.245	0.010	0.033	<u>0.988</u>	0.979	<u>0.059</u>	<u>0.185</u>	0.995	0.993

form of coherence that separate-then- transfer pipelines cannot enforce.

4.6. Scaling with Pseudo-Labeled Data

Whether paired supervision is strictly necessary is examined next. Since our content pipeline already uses an HT Demucs encoder, the same network doubles as a separator that produces pseudo-stems for arbitrary external mixtures at no extra cost. We train MixtureTT under five mixing ratios between paired CocoChorales data (\mathcal{D}_s) and pseudo-labeled external mixtures (\mathcal{D}_u), from fully paired to fully pseudo-labeled, holding the total training budget fixed.

5. Results

5.1. Main Results

Table 1 reports objective results on CocoChorales. Across both reconstruction and transfer settings, MixtureTT outperforms the two single-instrument baselines on every metric, despite an asymmetric input condition: the baselines receive ground-truth isolated stems while MixtureTT operates only on the polyphonic mixture. This directly substantiates our motivating claim—dedicated multi-instrument modeling matches and exceeds separate-then-transfer pipelines even when the latter are granted oracle separation as input, and does so without incurring cascaded separation error. A representative example is shown in Fig. 3.

The Single DiT ablation, matched in architecture and parameter count but with the cross-stem stage removed, isolates the contribution of joint denoising. Under identical inputs, the joint setting improves both per-stem quality and timbre metrics, and the gap widens at the mixture level: mixture-quality and harmonic-coherence metrics both benefit substantially from cross-stem attention, confirming that joint modeling of cross-stem dependencies is a core driver of generation quality rather than a mere efficiency choice.

The remaining two ablations characterize our disentanglement losses. Removing \mathcal{L}_{cls} preserves the low-dimensional bottleneck but eliminates explicit pressure against content–timbre leakage; the timbre-identity metric collapses while audio quality remains largely intact, confirming that the classifier adversary is what actually enforces disentanglement. Removing \mathcal{L}_{div} causes the four timbre embeddings to converge toward one another: the model still produces clean audio by distributional measures but can no longer discriminate between target instruments, exposing the collapse mode that the diversity loss is

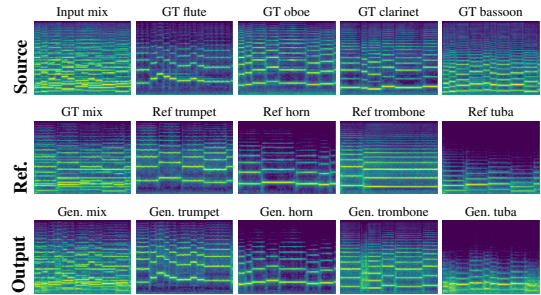


Figure 3: *Qualitative result of MixtureTT jointly generating the re-instrumented stems from an input mixture and four timbre references.*

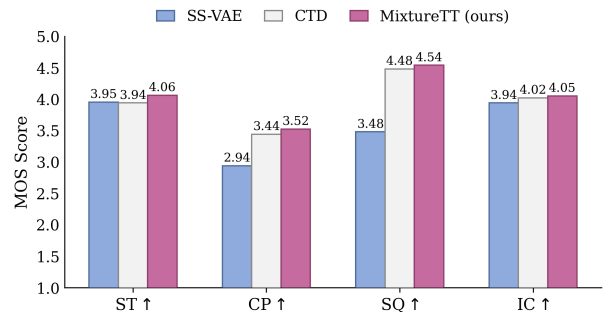


Figure 4: *Subjective MOS evaluation (1–5 scale).*

specifically designed to prevent.

5.2. Subjective Evaluation

The subjective study showing in Fig. 4 reinforces the objective picture. MixtureTT obtains the highest MOS on all four axes, despite both baselines receiving ground-truth isolated stems as input. The coherence margin is the most consequential of the four: IC measures precisely the form of ensemble-level consistency that separate-then-transfer pipelines have no mechanism to produce, and listeners rating our mixtures as more coherent than the mixdown of four independently transferred baseline stems constitutes direct perceptual validation of the joint formulation.

Table 2: Effect of supervision and data scale. \mathcal{D}_s : paired data; \mathcal{D}_u : external unpaired data.

	Sup.		Unsup.		Stem				Mix	
					FAD↓	JD↓	MFCC↓	Conf↑	FAD _m ↓	CCS↑
\mathcal{D}_s	100%	—	0%		0.255	0.245	0.033	0.979	0.185	0.993
\mathcal{D}_s	50%	\mathcal{D}_u	50%		0.261	0.285	0.031	0.972	0.194	0.909
\mathcal{D}_s	10%	\mathcal{D}_u	90%		0.273	0.326	0.032	0.964	0.205	0.882
\mathcal{D}_s	5%	\mathcal{D}_u	95%		0.286	0.334	0.033	0.958	0.209	0.871
—	0%	\mathcal{D}_u	100%		0.382	0.297	0.034	0.945	0.211	0.909

5.3. Scaling with Pseudo-Labeled Data

Table 2 reports performance when paired CocoChorales supervision is progressively replaced by pseudo-stems from our HT Demucs separator. All metrics remain close to the fully supervised model even when paired data drops to 10%, and the fully unsupervised setting still produces usable outputs with only moderate degradation. This indicates that MixtureTT can be trained with limited or no paired stems, opening the door to scaling beyond datasets where ground-truth separation is available.

Taken together, the objective, subjective, and scaling results confirm the three claims made in our introduction: that mixture-level per-stem timbre transfer is feasible without an explicit separation stage; that dedicated multi-instrument modeling outperforms the single-instrument paradigm even under a strictly harder input condition; and that joint cross-stem modeling is the key driver of quality at the mixture level.

6. Conclusion

This paper presented MixtureTT, a joint latent diffusion system for per-stem timbre transfer that operates directly on polyphonic mixtures. To our knowledge, this is the first system capable of flexibly re-instrumenting individual voices within a mixture without explicit source separation, query audio, or instrument labels. By jointly modeling per-stem content and cross-stem dependencies in a single diffusion pass, our joint stem diffusion transformer outperforms strong single-instrument baselines even under a strictly harder input condition, and a controlled ablation confirms cross-stem modeling as the key driver of this result. We leave to future work the extension to ensembles of varying size beyond the four-voice SATB setting, the integration of pseudo-labeled data at larger scales, and a closer study of how content-timbre disentanglement interacts with ensemble coherence. More broadly, we hope this work initiates a reflection on treating the polyphonic mixture as the natural object of study in generative music modeling, encouraging further exploration of mixture-level formulations across the broader family of music-manipulation tasks.

7. References

- [1] D. L. Wessel, “Timbre space as a musical control structure,” *Computer music journal*, pp. 45–52, 1979.
- [2] J. Engel, C. Resnick, A. Roberts, S. Dieleman, M. Norouzi, D. Eck, and K. Simonyan, “Neural audio synthesis of musical notes with wavenet autoencoders,” in *International conference on machine learning*. PMLR, 2017, pp. 1068–1077.
- [3] N. Mor, L. Wolf, A. Polyak, and Y. Taigman, “A universal music translation network,” *arXiv preprint arXiv:1805.07848*, 2018.
- [4] S. Huang, Q. Li, C. Anil, X. Bao, S. Oore, and R. B. Grosse, “Timbretron: A wavenet (cyclegan (cqt (audio))) pipeline for musical timbre transfer,” *arXiv preprint arXiv:1811.09620*, 2018.
- [5] G. Brunner, Y. Wang, R. Wattenhofer, and S. Zhao, “Symbolic music genre transfer with cyclegan,” in *2018 IEEE 30th international conference on tools with artificial intelligence (ictai)*. IEEE, 2018, pp. 786–793.
- [6] T. Kaneko and H. Kameoka, “Cyclegan-vc: Non-parallel voice conversion using cycle-consistent adversarial networks,” in *2018 26th European signal processing conference (EUSIPCO)*. IEEE, 2018, pp. 2100–2104.
- [7] O. Cifka, A. Ozerov, U. Şimşekli, and G. Richard, “Self-supervised vq-vae for one-shot music style transfer,” in *ICASSP 2021-2021 IEEE International Conference on Acoustics, Speech and Signal Processing (ICASSP)*. IEEE, 2021, pp. 96–100.
- [8] Y. Wu, Y. He, X. Liu, Y. Wang, and R. B. Dannenberg, “Transplayer: Timbre style transfer with flexible timbre control,” in *ICASSP 2023-2023 IEEE International Conference on Acoustics, Speech and Signal Processing (ICASSP)*. IEEE, 2023, pp. 1–5.
- [9] Y.-N. Hung, Y.-A. Chen, and Y.-H. Yang, “Learning disentangled representations for timbre and pitch in music audio,” *arXiv preprint arXiv:1811.03271*, 2018.
- [10] L. Comanducci, F. Antonacci, and A. Sarti, “Timbre transfer using image-to-image denoising diffusion implicit models,” *arXiv preprint arXiv:2307.04586*, 2023.
- [11] N. Demerlé, P. Esling, G. Doras, and D. Genova, “Combining audio control and style transfer using latent diffusion,” *arXiv preprint arXiv:2408.00196*, 2024.
- [12] M. Mancusi, Y. Halychanskyi, K. W. Cheuk, E. Moliner, C.-H. Lai, S. Uhlich, J. Koo, M. A. Martínez-Ramírez, W.-H. Liao, G. Fabbro *et al.*, “Latent diffusion bridges for unsupervised musical audio timbre transfer,” in *ICASSP 2025-2025 IEEE International Conference on Acoustics, Speech and Signal Processing (ICASSP)*. IEEE, 2025, pp. 1–5.
- [13] V. Popov, I. Vovk, V. Gogoryan, T. Sadekova, M. Kudinov, and J. Wei, “Diffusion-based voice conversion with fast maximum likelihood sampling scheme,” *arXiv preprint arXiv:2109.13821*, 2021.
- [14] M. Alinoori and V. Tzerpos, “Music-star: a style translation system for audio-based re-instrumentation,” in *ISMIR*, 2022, pp. 419–426.
- [15] T. Baoueb, X. Bie, H. Janati, and G. Richard, “Wavetransfer: A flexible end-to-end multi-instrument timbre transfer with diffusion,” in *2024 IEEE 34th International Workshop on Machine Learning for Signal Processing (MLSP)*. IEEE, 2024, pp. 1–6.
- [16] Y.-J. Luo, K. W. Cheuk, W. Choi, T. Uesaka, K. Toyama, K. Saito, C.-H. Lai, Y. Takida, W.-H. Liao, S. Dixon *et al.*, “Dismiss: Disentangling mixtures of musical instruments for source-level pitch and timbre manipulation,” *arXiv preprint arXiv:2408.10807*, 2024.
- [17] G. Mariani, I. Tallini, E. Postolache, M. Mancusi, L. Cosmo, and E. Rodolà, “Multi-source diffusion models for simultaneous music generation and separation,” *arXiv preprint arXiv:2302.02257*, 2023.
- [18] J. Ho, A. Jain, and P. Abbeel, “Denoising diffusion probabilistic models,” *Advances in neural information processing systems*, vol. 33, pp. 6840–6851, 2020.
- [19] Y. Song, J. Sohl-Dickstein, D. P. Kingma, A. Kumar, S. Ermon, and B. Poole, “Score-based generative modeling through stochastic differential equations,” *arXiv preprint arXiv:2011.13456*, 2020.
- [20] R. Rombach, A. Blattmann, D. Lorenz, P. Esser, and B. Ommer, “High-resolution image synthesis with latent diffusion models,” in *Proceedings of the IEEE/CVF conference on computer vision and pattern recognition*, 2022, pp. 10 684–10 695.
- [21] H. Liu, Z. Chen, Y. Yuan, X. Mei, X. Liu, D. Mandic, W. Wang, and M. D. Plumbley, “Audioldm: Text-to-audio generation with latent diffusion models,” *arXiv preprint arXiv:2301.12503*, 2023.

- [22] Z. Evans, J. D. Parker, C. Carr, Z. Zukowski, J. Taylor, and J. Pons, “Stable audio open,” in *ICASSP 2025-2025 IEEE International Conference on Acoustics, Speech and Signal Processing (ICASSP)*. IEEE, 2025, pp. 1–5.
- [23] T. Karras, M. Aittala, T. Aila, and S. Laine, “Elucidating the design space of diffusion-based generative models,” *Advances in neural information processing systems*, vol. 35, pp. 26 565–26 577, 2022.
- [24] J. Ho and T. Salimans, “Classifier-free diffusion guidance,” *arXiv preprint arXiv:2207.12598*, 2022.
- [25] D. Yang, J. Tian, X. Tan, R. Huang, S. Liu, X. Chang, J. Shi, S. Zhao, J. Bian, X. Wu *et al.*, “Uniaudio: An audio foundation model toward universal audio generation,” *arXiv preprint arXiv:2310.00704*, 2023.
- [26] K. Wang, W. Guan, Z. Jiang, H. Huang, P. Chen, W. Wu, Q. Hong, and L. Li, “Discl-vc: Disentangled discrete tokens and in-context learning for controllable zero-shot voice conversion,” in *Proc. Interspeech 2025*, 2025, pp. 1383–1387.
- [27] J. Zhao, X. Wang, and Y. Wang, “Prosody-Adaptable Audio Codecs for Zero-Shot Voice Conversion via In-Context Learning,” in *Interspeech 2025*, 2025, pp. 4893–4897.
- [28] J. Zhao, W. Zeng, T. Lyu, and Y. Wang, “Comelsinger: Discrete token-based zero-shot singing synthesis with structured melody control and guidance,” *IEEE Transactions on Audio, Speech and Language Processing*, 2026.
- [29] A. Caillon and P. Esling, “Rave: A variational autoencoder for fast and high-quality neural audio synthesis,” *arXiv preprint arXiv:2111.05011*, 2021.
- [30] R. Kumar, P. Seetharaman, A. Luebs, I. Kumar, and K. Kumar, “High-fidelity audio compression with improved rvqgan,” *Advances in Neural Information Processing Systems*, vol. 36, pp. 27 980–27 993, 2023.
- [31] S. Rouard, F. Massa, and A. Défossez, “Hybrid transformers for music source separation,” in *ICASSP 2023-2023 IEEE International Conference on Acoustics, Speech and Signal Processing (ICASSP)*. IEEE, 2023, pp. 1–5.
- [32] E. Perez, F. Strub, H. De Vries, V. Dumoulin, and A. Courville, “Film: Visual reasoning with a general conditioning layer,” in *Proceedings of the AAAI conference on artificial intelligence*, vol. 32, no. 1, 2018.
- [33] W. Peebles and S. Xie, “Scalable diffusion models with transformers,” in *Proceedings of the IEEE/CVF international conference on computer vision*, 2023, pp. 4195–4205.
- [34] Y. Wu, J. Gardner, E. Manilow, I. Simon, C. Hawthorne, and J. Engel, “The chamber ensemble generator: Limitless high-quality mir data via generative modeling,” *arXiv preprint arXiv:2209.14458*, 2022.
- [35] I. Loshchilov and F. Hutter, “Decoupled weight decay regularization,” *arXiv preprint arXiv:1711.05101*, 2017.
- [36] K. Kilgour, M. Zuluaga, D. Roblek, and M. Sharifi, “Fr\`echet audio distance: A metric for evaluating music enhancement algorithms,” *arXiv preprint arXiv:1812.08466*, 2018.
- [37] M. Mauch and S. Dixon, “pyin: A fundamental frequency estimator using probabilistic threshold distributions,” in *2014 IEEE international conference on acoustics, speech and signal processing (icassp)*. IEEE, 2014, pp. 659–663.
- [38] G. Richard, S. Sundaram, and S. Narayanan, “An overview on perceptually motivated audio indexing and classification,” *Proceedings of the IEEE*, vol. 101, no. 9, pp. 1939–1954, 2013.